

A unified approach for detection of induced epileptic seizures in rats using ECoG signals

M. Niknazar^{a,*}, S.R. Mousavi^a, S. Motaghi^b, A. Dehghani^b, B. Vosoughi Vahdat^a, M.B. Shamsollahi^a, M. Sayyah^b, S.M. Noorbakhsh^b

^a Biomedical Signal and Image Processing Laboratory (BISPL), School of Electrical Engineering, Sharif University of Technology, P.O. Box 11365-9363, Tehran, Iran

^b Physiology and Pharmacology Department, Pasteur Institute of Iran, Tehran, Iran

ARTICLE INFO

Article history:

Received 6 October 2012

Revised 23 January 2013

Accepted 29 January 2013

Available online xxxx

Keywords:

Induced epilepsy

Epileptic rat

Seizure detection

Seizure onset estimation

Pentylentetrazole (PTZ)

ABSTRACT

Objective: Epileptic seizure detection is a key step for epilepsy assessment. In this work, using the pentylentetrazole (PTZ) model, seizures were induced in rats, and ECoG signals in interictal, preictal, ictal, and postictal periods were recorded. The recorded ECoG signals were then analyzed to detect epileptic seizures in the epileptic rats.

Methods: Two different approaches were considered in this work: thresholding and classification. In the thresholding approach, a feature is calculated in consecutive windows, and the resulted index is tracked over time and compared with a threshold. The moment the index crosses the threshold is considered as the moment of seizure onset. In the classification approach, features are extracted from before, during, and after ictal periods and statistically analyzed. Statistical characteristics of some features have a significant difference among these periods, thus resulting in epileptic seizure detection.

Results: Several features were examined in the thresholding approach. Nonlinear energy and coastline features were successful in epileptic seizure detection. The best result was achieved by the coastline feature, which led to a mean of a 2-second delay in its correct detections. In the classification approach, the best result was achieved using the fuzzy similarity index that led to $P_{\text{value}} < 0.001$.

Conclusion: This study showed that variance-based features were more appropriate for tracking abrupt changes in ECoG signals. Therefore, these features perform better in seizure onset estimation, whereas nonlinear features or indices, which are based on dynamical systems, can better track the transition of neural system to ictal period.

Significance: This paper presents examination of different features and indices for detection of induced epileptic seizures from rat's ECoG signals.

© 2013 Elsevier Inc. All rights reserved.

1. Introduction

Epilepsy is a bewildering neurological disorder that may cause brief electrical disturbances in the brain producing changes in sensation, awareness and behavior [1]. Epileptic seizures reflect the clinical signs of an excessive and hyper-synchronous activity of neurons in the brain [56]. Epilepsy is a neurological disease that directly affects 50 million people worldwide [57]. In about two thirds of patients with epilepsy, seizures can be satisfactorily controlled with currently available antiepileptic drugs [58]. Another 8% can benefit

from epilepsy surgery. Unfortunately, seizures in the remaining 25% of patients with epilepsy cannot be treated sufficiently by any available therapy [2]. Epileptic seizure detection would help these people to have a convenient life. Since an epileptic seizure is related to the electrical activity of brain, the electroencephalogram (EEG) signal is a useful biosignal for epileptic seizure detection. Indeed, epilepsy is characterized by recurrent seizures that are observable in the EEG signal [3]. When an epileptic focal seizure is generated, synchronized epileptic brain activity is initially observed in a small area of the brain. From this focus, the activity spreads to other brain areas [4]. This process is reflected in the recorded EEG. However, there is very little confirmed knowledge of the exact mechanism(s) by which this occurs [5]. Conventional seizure detection methods such as visual inspection of the EEG by a trained neurologist are challenging because of the presence of myogenic artifacts. Furthermore, visual inspection of the EEG data has not been found to be reliable in detecting the characteristic changes that precede seizure onsets [4]. Over the years, many researchers have attempted to develop algorithms for automatic

* Corresponding author.

E-mail addresses: niknazar@alum.sharif.edu (M. Niknazar), moosavir@alum.sharif.edu (S.R. Mousavi), sahelmotaghi@uk.ac.ir (S. Motaghi), yasad490@yahoo.com (A. Dehghani), vahdat@sharif.edu (B. Vosoughi Vahdat), mbshams@sharif.edu (M.B. Shamsollahi), sayyahm2@pasteur.ac.ir (M. Sayyah), smn2133@columbia.edu (S.M. Noorbakhsh).

analysis of EEGs to recognize epileptiform transients and to efficiently process data produced by long-term EEG recordings [6,7].

The early methods of automatic EEG processing were simple analysis of EEG signals in the time or frequency domain. Mimetic techniques have been widely used for detecting epileptiform discharges [6,8,9]. They were based on breaking the EEG signal into half-waves and measuring duration, amplitude, and sharpness (second derivative) of the peaks relative to the background. These measures were then combined to decide whether a half-wave is a potential spike or sharp wave or not. Detecting the spikes and sharp waves is possible when the signal has no artifacts. However, artifacts caused by electromyogram (EMG) activity and other EEG activities resembling spikes caused these methods to fail [10].

Spectral approach is another approach based on earlier observations that the EEG spectrum contains characteristic waveforms clustered in four distinct frequency bands. Such methods have been proved beneficial for EEG characterization, but earlier methods based on fast Fourier transform (FFT) suffer from large noise sensitivity [38]. Newer parametric methods for power spectrum estimation such as the autoregressive (AR) technique reduce the spectral loss issues and give better frequency resolution [11]. However, since EEG signals are non-stationary, parametric methods are not suitable for frequency decomposition of these signals [39]. Time-frequency and wavelet transforms were also used to analyze EEG signals of patients with epilepsy [12].

Some other seizure detection methods are based on artificial neural networks (ANNs) [13,14,9]. ANNs have offered an attractive solution for recognition and classification tasks where the rules are not clear [40]. Nonetheless, ANNs require various training sets to reduce the influence of artifacts and the training of such networks is troublesome and unrealistic for real-life systems [9].

Studies in seizure detection vary in their theoretical approaches, validation of results, and amount of data analyzed. Some relative weaknesses in this literature are the lack of extensive testing on baseline data free from seizures, and the lack of technically rigorous validation and quantification of algorithm performance in many studies. In recent years, attempts in seizure detection and prediction from EEG analysis have been mostly based on two approaches: 1) Examination of the waveforms in the seizure-free EEG to find markers or changes in neuronal activity such as spikes which may be precursors to seizures; 2) Analysis of the nonlinear spatio-temporal evolution of EEG signals to find a governing rule as the system moves from a seizure-free to seizure state [15]. Recurrence quantification analysis (RQA) [16] and similarity index methods [17,37] are among the second approach.

To validate seizure detection methods, various animal models are used. The most popular and widely used models are the maximal electroshock seizure test and the subcutaneous (s.c.) pentylenetetrazole (PTZ) test [18,45,46,59,60]. Development of various new antiepileptic drugs is primarily based on these two seizure models [18]. The s.c. PTZ test is used to find drugs effective against generalized absence seizures [18]. People with absence epilepsy have repeated seizures that cause momentary lapses of consciousness. These sudden and abrupt seizures most commonly occur in childhood or adolescence and may have significant impact on educational development [19].

In [51], seizure-triggered trigeminal nerve stimulation has been employed to reduce PTZ-induced seizure activity in awake rats. In another recent study, feasibility of an automatic seizure control system in rats with PTZ-induced seizures was investigated through single and multiple stimulations [52]. Prior to applying the stimulation, an automatic seizure detector is needed. Several algorithms have been proposed to detect PTZ-induced seizures. A cumulative sum algorithm was proposed in [44] to detect such seizures. This feature was then combined with the general likelihood ratio test to improve the accuracy [53]. Among several other features used for PTZ-induced seizure detection, are cross-bicoherence gain [46] and cross-correlation variance [50]. In addition to EEG, vagus electroneurogram (VENG) [47], optical coherence tomography (OCT) [48], and Laplacian EEG [45] were also

used to analyze and detect PTZ-induced seizures in rats. There are also some studies on the prediction of PTZ-induced seizures in rats. In [49], a new wavelet-based residual entropy method was employed to measure entropy of cortical and subcortical field potentials for seizure prediction.

The goal of this study was to detect clonic seizures in rats with induced by s.c. injection of PTZ. The electrocorticography (ECoG) signals in interictal, preictal, ictal and postictal periods have been recorded and analyzed. This paper presents a unified approach for detection of induced seizures in rats using ECoG signals.

2. Dataset

Data used in this study were collected at Pasteur Institute of Iran from male Wistar rats weighing 200–250 g. These rats were kept in a controlled environment (6 am/6 pm light/dark cycle; 22 ± 1 °C) and freely had access to food and water. Two screw electrodes were inserted into the skull over the frontal and occipital cortex under ketamine (60 mg/kg, i.p.) and xylazine (10 mg/kg, i.p.) anesthesia. The epidural electrodes were fixed on the skull using dental acrylic and an extra screw. The animals were allowed 3 days for recovery and handled gently to be adapted with the recording procedure. ECoG was then recorded in the control group for 60 min. For the test group, ECoG signal was recorded a few minutes before the administration of a convulsive dose of pentylenetetrazole (60 mg/kg). PTZ was injected s.c. to freely moving rats through a polyethylene tube. Electrical activity was then recorded for 60 min. All measurements and injections took place between 10:00 and 15:00 h. ECoG signals were amplified by an AC differential amplifier (DAM 80, WPI) with gain of 1000 and with band-pass filter setting of 0.1–1000 Hz. The sampling rate was 10 kHz, and the analog-to-digital conversion was performed at 12-bit resolution. The ECoG dataset was downsampled to 1 kHz, and preprocessed by a 50-Hz notch filter and a low pass 60-Hz filter. The analyzed dataset consisted of 12 rats in the test group and 15 rats in the control group. The data of 6 rats in the test group had some issues due to sudden rat movements, amplifier saturation, and severe noise due to the data acquisition system. Therefore, we had to cut some parts of the starting segments or ending segments of data from these 6 rats. Nevertheless, for the remaining parts of data from these 6 rats, the signals were continuous, i.e. excluded segments were always at the beginning or the end of the signals, not in the middle of them. Data from these 6 rats were not used in the seizure onset estimation section, because although some segments of the beginning or the end of these data have been cut, remaining parts are still too noisy to perform accurate evaluation of the algorithms. Data from these 6 rats have been used only in the classification section.

Seizure onset in each experiment was determined by an experienced experimental scientist by observation of animal behavior including head nodding and general clonus of the whole body [20], which corresponds to the score of 3 (myoclonic jerk) by Racine's seizure scoring system [54]. PTZ initially produces myoclonic jerks, which subsequently become sustained and may lead to generalized tonic-clonic seizures [61]. After some minutes, the behavior of rats becomes normal again and there would be no behavioral signs of the Racine scale. A return to normal behavior was the criterion for determining the end of the seizure. The injection time, seizure onset time and seizure end time of experiments for unsharpened data are shown in Table 1.

3. Materials and methods

In this section, various methods for analyzing epileptiform EEG signals in different approaches are introduced. These methods are also applicable to ECoG signals. In the first subsection, two main approaches for seizure detection are described in detail. Then, in the next subsection, a wide range of features and indices that vary from simple to complex are

Table 1
The Time Recording of Each Experiment.

Rat no.	Injection time	Seizure onset	Seizure end
1	21:34	29:02	30:35
2	10:33	3:09	16:24
3	6:05	9:18	9:36
4	7:16	20:05	20:36
5	5:55	21:25	22:39
6	5:11	9:59	11:01

The time format is minute:second Starting time is always from 00:00.

presented. Most of these features and indices have been already used in the literature for epileptiform EEG analysis. In this study, a few new features and indices are also introduced. The aim of this study was to determine how each feature or index is suitable for seizure detection of the acquired data adopting each main approach.

3.1. Different approaches for detection of induced seizures

Recorded EEG of seizure activity can be characterized by four stages: (1) the ictal stage that starts at the seizure onset and finishes at the seizure end; (2) the postictal stage which is the period following the seizure end and represents a return to normal background activity; (3) the interictal stage which is the period between the postictal stage of one seizure and the moments before the next seizure onset, and (4) the preictal stage which is the moment right before the seizure onset. In this section, two general approaches for detecting seizures in EEG signals are introduced.

3.1.1. First approach for seizure detection: Thresholding

In this approach, a feature or index is calculated for each consecutive window of an EEG recording and the moment of seizure onset is

estimated by comparing this feature or index with a threshold. Fig. 1 shows the sliding window analysis schematically.

In order to define the threshold in this approach, the first step is to calculate the mean value μ and standard deviation (S.D.) σ of each feature or index during the interictal phase. The second step is to determine a pattern for ictal phase detection. A common pattern is a local rise characterized by height k and duration d . The height of the rise k can be obtained in units of the S.D. of the baseline epoch, then the threshold value can be set to $(\mu + k\sigma)$, where its duration d can be quantified by the time during which the value of a profile rises over this threshold [31]. During practical implementation of this detection method, a backward moving-average filter is first applied to smooth the profile of each feature or index to avoid abrupt variations. Then the time when the smoothed values of each feature or index exceed the threshold value $(\mu + k\sigma)$ for the first time and remain over it within duration d is considered as detection point. Decreasing the parameter k decreases the detection threshold value $(\mu + k\sigma)$ and therefore increases sensitivity and decreases delay time. On the other hand, it also leads to more false positives. Considering this trade-off, sensitivity and delay time should be evaluated in conjunction with the false detection rate. The parameters k and d govern the mean height of a rise over a certain time and the threshold for ictal phase detection. The parameters k and d are optimized for the whole dataset (including test group and control group) to maximize the detection performance. The performance Q of the detection method is defined as [31]:

$$Q = \sqrt{\frac{Se^2 + Sp^2}{2}} \quad (1)$$

where Se is the sensitivity, defined as fraction of correct detections to all seizures; Sp is the specificity rate, defined as 1 minus the average

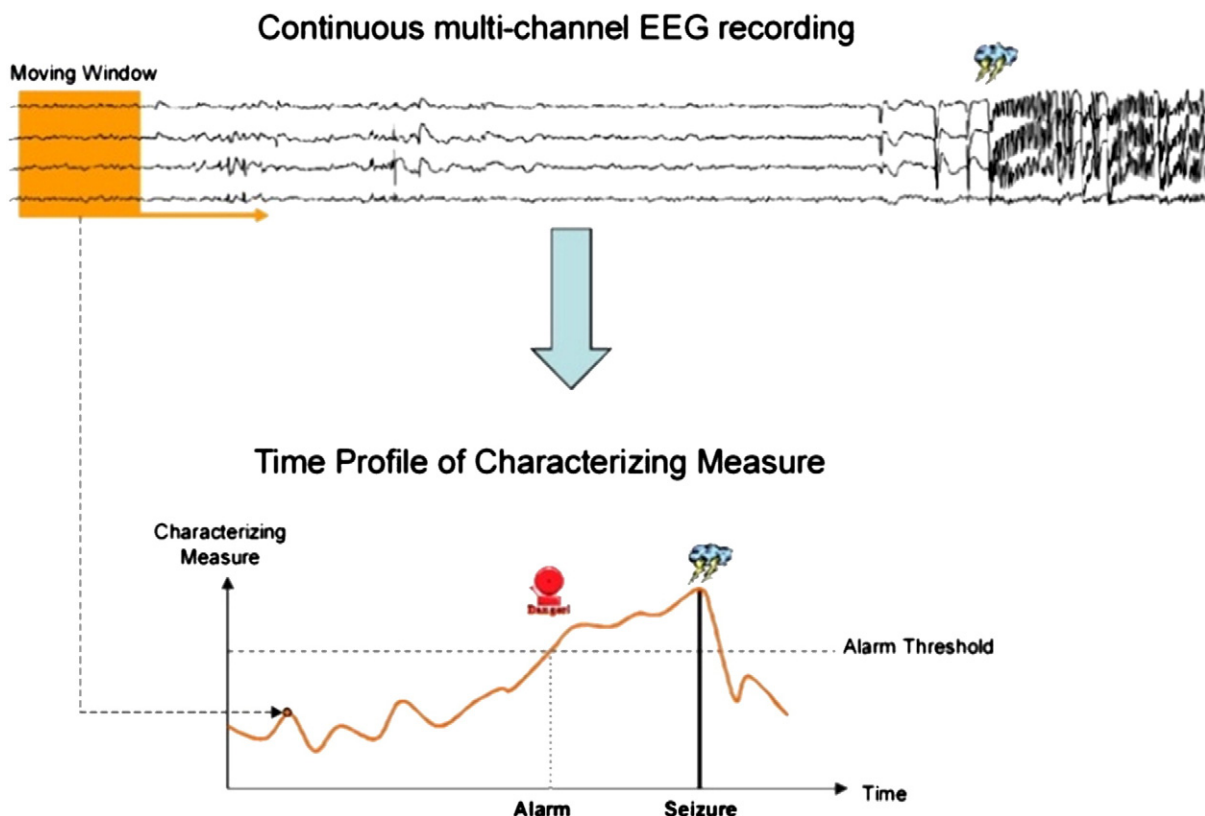


Fig. 1. Continuous multi-channel EEG recordings are analyzed by means of a moving-window analysis. The data covered by the orange window is transformed into a single value in the index of a multivariate characterizing measure. When this index crosses a certain pre-defined threshold, an alarm is issued.

number of false positive detections per hour of interictal EEG in test and control groups (for more than 1 false positive per hour, Sp is set to zero).

3.1.2. Second approach for seizure detection: Classification

There are some problems with seizure detection using thresholding. Determining a threshold for seizure onset detection is a challenging problem. The reason is that a seizure is a transient occurrence of signs and/or symptoms due to abnormal excessive or synchronous neuronal activity in the brain [41]. This significantly suppresses seizure onset estimation accuracy, as the seizure itself is a transient occurrence, not a binary occurrence. Therefore, most of the time, we try to find a feature or index the mean of which significantly changes before, during, and after seizure intervals. In this approach, there is no need to define threshold and the important requirement is that a valid statistical analysis shows that the mean variations in these intervals are significant. In fact, this issue is a classification problem with two classes, during seizure class and out of seizure class.

3.2. Features and indices

According to [21], features or indices for epileptiform EEG analysis can be extracted using time domain techniques, frequency domain techniques and nonlinear techniques. This does not mean that all time domain and frequency domain techniques are linear but means they are not based on the theories of dynamical systems.

3.2.1. Time domain features

Features extracted from time domain techniques are fast and simple. They have been used in seizure detection and in sleep research as well [21,42].

3.2.1.1. Local variance. This feature is also called activity and is equal to the variance of signal in the present window. When the power of noise is high relative to that of the signal, this feature is not useful for analysis [22].

3.2.1.2. Mobility. This feature is defined as the standard deviation of the first derivative of signal to that of the original signal, and mathematically can be expressed as [21]:

$$mobility = \frac{\sigma_{s'}}{\sigma_s} \tag{2}$$

where σ is standard deviation and $s'(n) = s(n + 1) - s(n)$.

3.2.1.3. Complexity. This feature is defined as the ratio of the mobility of the first derivative of signal to the mobility of signal [21]:

$$complexity = \frac{\sigma_{s''}/\sigma_{s'}}{\sigma_{s'}/\sigma_s} \tag{3}$$

3.2.1.4. Coastline. This feature is defined as the sum of the absolute values of distances from one data point to the next and can be expressed as [22]:

$$coastline = \sum_{n=2}^N |s(n) - s(n-1)| \tag{4}$$

where $|\cdot|$ presents the absolute value operator and N is the number of data points in the present window. This feature is based on the fact that during a seizure, signal is relatively high-amplitude and high frequency. It fails in case of large amplitude noise. It also fails when the amplitude of signal during a seizure is less than that of the normal interval [22].

3.2.1.5. Autocorrelation. Seizures can be detected even when data points are somehow compressed [22]. In this method, data points of the present window N are initially divided into n segments, so that S_i is one of these segments. Then i -th high value and i -th low value are computed as:

$$HV_i = \min[\max(S_i), \max(\max(S_{i+1}), \max(S_{i+2}))] \tag{5}$$

$$LV_i = \max[\min(S_i), \min(\min(S_{i+1}), \min(S_{i+2}))] \tag{6}$$

Two features can be extracted from this formulation:

$$\sum_{i=1}^{N/n-2} (HV_i - LV_i) \tag{7}$$

and

$$\sum_{i=1}^{N/n-2} \left(\frac{HV_i - LV_i}{\max(S_i) - \min(S_i)} \right) \tag{8}$$

In the case where significant EEG autocorrelation is present, these two features have large values. Although Eq. (7) is normalized to the range of the index pixel and hence is more indicative of the actual autocorrelation, the denominator in the equation may make it more susceptible to low-amplitude and high-frequency noise, which results in a significantly decreased specificity [22].

3.2.1.6. Nonlinear energy. This feature is defined as follows:

$$NE = \frac{1}{N-2} \sum_{n=2}^{N-1} (s^2(n) - s(n-1)s(n+1)) \tag{9}$$

where N is number of data points in the present window.

3.2.2. Frequency domain features

These techniques include features of frequency domain using Fourier transform. These features are relatively more complicated than time domain features and are usually used for seizure-related EEG classification.

3.2.2.1. Spectral skewness. Skewness (or normalized skewness) is a measure in statistics and is defined as:

$$skewness = \frac{E(S-\eta)^3}{\sigma^3} \tag{10}$$

where $E(x)$ is the mathematic expectation of random variable x and S represents the amplitude of FFT coefficient of EEG signal in the present window. η and σ are mean and standard deviation of S , respectively. Skewness is a measure of the asymmetry of the probability distribution of a real-valued random variable.

3.2.2.2. Spectral kurtosis. Kurtosis (or normalized kurtosis) is another measure in the statistics and is defined as:

$$kurtosis = \frac{E(S-\eta)^4}{\sigma^4} \tag{11}$$

Kurtosis is a measure of the peakedness of the probability distribution of a real-valued random variable. Higher kurtosis means that the variance is mostly the result of infrequent extreme deviations, as opposed to frequent modestly sized deviations.

3.2.2.3. Spectral entropy. In information theory, entropy is a measure of the uncertainty associated with a random variable. For calculating

spectral entropy, first the amplitude spectrum obtained from FFT has to be normalized. Then using the classical Shannon entropy [23], the spectral entropy is defined as:

$$Entropy = - \sum_{i=1}^N |S(i)| \log_2 |S(i)| \tag{12}$$

3.2.3. Nonlinear features

Recent studies suggest that EEG signals are multivariate time series that stem from highly nonlinear and multidimensional systems [24]. As a result, one of the most important recent approaches for analyzing epileptiform EEGs is using nonlinear methods for analysis of the nonlinear spatio-temporal evolution of the EEG signals to find a governing rule as the system moves from a seizure-free to seizure state [15]. Nonlinear techniques are more complicated than time domain and frequency domain techniques and are usually used for seizure-related EEG classification and seizure detection and prediction [43]. A single record from a dynamic system is the outcome of all interacting variables of the system and thus, in principle, should contain information about the dynamics of all significant variables involved in the operation of the system [25]. Dynamic systems can be described by a set of states and transition rules, which specify how the system may proceed from one state to another. Each state is the state of all independent variables involved in operation of the system that is defined as a vector. Vectors of different states make a vector space called phase space. Then the dynamics of the system can be studied by examining the dynamics of the corresponding vectors in the phase space [21]. However, in experimental situations, not all relevant components to construct the state vector are known or measurable. Often a discrete-time measurement of only one observable quantity is available. This yields scalar discrete-time series $s_i = s(i\Delta t)$. In such a case, the phase space has to be reconstructed. A frequently used method for the reconstruction is the time delay method proposed by Takens [26], in which phase space is reconstructed by its trajectories:

$$x_k = (s_k, s_{k+\tau}, \dots, s_{k+(m-1)\tau}), \tag{13}$$

where $k = 1, 2, \dots, N - (m - 1)\tau$, N is the total number of data points in the present window, m is embedding dimension, and τ is time delay.

For finite and noisy datasets like EEG recordings, m and τ of the trajectories should be carefully determined. The most common method for choosing a proper time delay is based on the detection of the first local minimum of the mutual information (MI) function [27], since the first minimum of the $MI(\tau)$ portrays the time delay where the signals $(s_\tau, s_{\tau+1}, \dots, s_{L-\tau})$ and $(s_{\tau+\tau}, s_{\tau+\tau+1}, \dots, s_L)$ have the minimal overlapping information. After the selection of the optimum lag, the minimum embedding dimension was determined based on Cao's method. The method was applied repeatedly starting with a low value of the embedding dimension m and then increasing it until the number of false neighbors decreases to zero [28].

3.2.3.1. Recurrence quantification analysis. The recurrence of states is a fundamental property of a dynamical system [29]. Recurrence plots (RP), proposed by Eckmann et al. [30], can describe the recurrence property of a dynamical system. The key step of RP is to calculate the following $N \times N$ matrix:

$$R_{ij}(\varepsilon) = \Theta(\varepsilon - \|x_i - x_j\|) \tag{14}$$

where $\Theta(x)$ is the Heaviside function [55] and $\| \cdot \|$ is the norm (e.g., Euclidean norm) operator. The cutoff distance ε defines a sphere centered at x_i and determines if x_j falls within this sphere. In this work, $\varepsilon = 1.5$ was chosen (in unit of standard deviation σ) [16]. The recurrence plot of each dynamical system has its own topology [26]. This

topology can be quantified by RQA. Measures of RQA are based on recurrence point density, the diagonal line structures and the vertical line structures.

3.2.3.1.1. Measures based on the recurrence density. The simplest measure of the RQA is the recurrence rate (RR):

$$RR = \frac{1}{N^2} \sum_{i,j=1}^N R_{ij}(\varepsilon) \tag{15}$$

which is a measure of the density of recurrence points in the RP. In the limit $N \rightarrow \infty$ RR is the probability that a state recurs to its ε -neighborhood in phase space [26].

3.2.3.1.2. Measures based on diagonal lines. These measures are based on the histogram $P(l)$ of diagonal lines of length l . Processes with uncorrelated or weakly correlated, stochastic or chaotic behavior cause none or very short diagonals, whereas deterministic processes cause longer diagonals and less single, isolated recurrence points [26]. Therefore, the ratio of recurrence points that form diagonal structures (of at least length l_{min}) to all recurrence points is introduced as a measure for determinism (or predictability) of the system:

$$DET = \frac{\sum_{l=l_{min}}^N lP(l)}{\sum_{l=1}^N lP(l)} \tag{16}$$

The threshold l_{min} excludes the diagonal lines, which are formed by the tangential motion of the phase space trajectory. However, we have to take into account that the histogram $P(l)$ can become sparse if l_{min} is too large, and, thus, the reliability of DET decreases. Thereby, as in [19], we adopted $l_{min} = 2$ in our study.

A diagonal line of length l means that a segment of the trajectory is rather close during l time step to another segment of the trajectory at a different time; thus, these lines are related to the divergence of the trajectory segments. The average diagonal line length is the average time that two segments of the trajectory are close to each other, and can be interpreted as the mean prediction time:

$$L = \frac{\sum_{l=l_{min}}^N l^2 P(l)}{\sum_{l=l_{min}}^N l P(l)} \tag{17}$$

The measure entropy refers to the Shannon entropy [23] of the probability $p = P(l)/N_l$ to find a diagonal line of exactly length l in the RP:

$$ENTR = - \sum_{l=l_{min}}^N p(l) \ln p(l) \tag{18}$$

ENTR reflects the complexity of the RP with respect to the diagonal lines, e.g. for uncorrelated noise the value of ENTR is rather small, indicating its low complexity.

3.2.3.1.3. Measures based on vertical lines. These measures are based on the histogram $P(v)$ of vertical lines of length v . The ratio between the recurrence points forming the vertical structures and the entire set of recurrence points is called laminarity:

$$LAM = \frac{\sum_{v=v_{min}}^N vP(v)}{\sum_{v=1}^N vP(v)} \tag{19}$$

The computation of LAM is realized for those v that exceed a minimal length v_{min} in order to decrease the influence of the tangential motion. For recurrence maps, $v_{min} = 2$ is an appropriate value [26]. LAM represents the occurrence of laminar states in the system without describing the length of these laminar phases. It will decrease if the RP consists of more single recurrence points than vertical structures.

The average length of vertical structures is called trapping time:

$$TT = \frac{\sum_{v=v_{\min}}^N vP(v)}{\sum_{v=v_{\min}}^N P(v)} \quad (20)$$

TT estimates the mean time that the system will abide at a specific state or how long the state is trapped.

It is worth noting that RQA does not require any assumption about noise, linearity, stationarity and length of signal [24].

3.2.3.2. Fractal dimension. The fractal dimension can be a measure of signal complexity. The degree of complexity of a signal increases with the dimension [21]. In this study, Higuchi's algorithm was used for calculating the fractal dimension [32]. From a given time series, $s(n)$, $n = 1, \dots, N$, first x_m^k for $m = 1, 2, \dots, k$ is constructed as:

$$x_m^k = (s_m, s_{m+k}, s_{m+2k}, \dots, s_{m+\lfloor \frac{N-m}{k} \rfloor k}) \quad (21)$$

where the notation $\lfloor \cdot \rfloor$, means rounding the argument down to the nearest integer. Then $L_m(k)$ can be defined as the length of each x_m^k :

$$L_m(k) = \frac{1}{k} \sum_{i=1}^{\lfloor (N-m)/k \rfloor} |s(m+ik) - s(m+(i-1)k)| \frac{n-1}{\lfloor \frac{N-m}{k} \rfloor k} \quad (22)$$

For each time interval k the length of the corresponding curve, $L(k)$, is defined to be the mean of the values $L_m(k)$ for $m = 1, \dots, k$. If $L(k)$ is proportional to k^{-D} , then the curve is fractal-like with the dimension D .

3.2.3.3. Approximate entropy. Like all entropies, approximate entropy describes the amount of regularity in the data. A smaller value of approximate entropy indicates behavior that is more regular. In this study, the algorithm presented by Pincus et al. [33] based on the Kolmogorov–Sinai entropy was used. First, vector x_i for $1 \leq i \leq N - m + 1$ is constructed from $s(n)$, $n = 1, \dots, N$:

$$x_i = (s(i), \dots, s(i+m-1)) \quad (23)$$

Then using a fixed real positive number r , for each index i a correlation sum $C_i^m(r)$ is constructed as:

$$C_i^m(r) = \frac{\text{number of } x_j \text{ such that } d(x_i, x_j) \leq r}{N-m+1} \quad (24)$$

where $d(x_i, x_j)$ means the distance between two vectors; the Euclidean norm is used as a distance measure in this study. Next $\Phi^m(r)$ is defined as:

$$\Phi^m(r) = \frac{1}{N-m+1} \sum_{i=1}^{N-m+1} \ln C_i^m(r) \quad (25)$$

and finally the approximate entropy is:

$$ApEn = \Phi^m(r) - \Phi^{m+1}(r) \quad (26)$$

In this study, parameter r has been chosen as suggested by Pincus et al. [33], meaning that the value of r was $0.2\sigma_s$, where σ_s is the standard deviation of the s .

3.2.3.4. Maximal Lyapunov exponent. The Lyapunov exponents provide a possible way to measure chaos. If the system exhibits sensitive dependence on initial conditions, then after a slight disturbance the system follows a different path than it would have followed without the disturbance. In the case of a positive Lyapunov exponent, these paths diverge exponentially [21]. There are many different methods for calculating Lyapunov exponents in the literature. The method used in

this study is based on the algorithm presented by Kantz and Schreiber [34]. In this algorithm, a point in the phase space is chosen and all its neighbors closer than a positive constant value are selected. Then the average distance over all neighbors is computed as a function of time. Now the logarithm of the average distance is an expansion rate over that time. Repeating this process for many different starting times and taking an average, we get a value, which we denote by $S(\Delta t)$. Since the minimum embedding dimension or the optimal neighborhood size may be unknown for a given dataset, the values $S(\Delta t)$ have to be calculated for several embedding dimension and neighborhood size pairs to see if for some time range of Δt the function $S(\Delta t)$ exhibits a linear increase. If this is the case, then the slope is the estimate for the maximal Lyapunov exponent per time step [21].

3.2.3.5. Dynamical similarity index. One of the most common nonlinear methods that analyzes the nonlinear spatio-temporal evolution of the EEG signals to find the transition from a seizure-free to seizure state is called dynamical similarity index [35] based on nonlinear time series proposed by Baulac and Varela [34]. The method consists of the reconstruction of EEG dynamics that uses time intervals between two positive zero crossings and the measurement of similarity between dynamics from a reference windowed state S_{ref} and a present one S_t . Reference windows should be recorded during an interval quite distant in time from any seizure. Then trajectory matrix is constructed from the vectors in the phase space that contains the complete record of patterns that have occurred within a window. For example, given a time series x_n , where $n = 1, 2, \dots, N_n$, the trajectory or augmented matrix A may be constructed as:

$$A_{ij} = x_{j+(i-1)r} \quad (27)$$

where $1 \leq i \leq m$ and $1 \leq j \leq N = N_n - (m-1)r$. m is the dimension of the phase space and r , a natural number is the time difference between the elements. The trajectory matrix has dimensions m by N . To reduce noise, the trajectory matrices $A(S_t)$ of the sliding window and $A(S_{ref})$ of the reference window are projected on the principal axes of the reference window, yielding $X(S_t)$ and $A(S_{ref})$, respectively, by means of a singular value decomposition (SVD) of the reference window [17]. To achieve a significant reduction in the volume of data without loss of potentially valuable dynamical information, a random selection $Y(S_{ref})$ of $X(S_{ref})$ in the phase space is selected [17]. In this study, the size of $Y(S_{ref})$ was chosen equal to the size of $X(S_t)$. The second step is to compare $Y(S_{ref})$ with $X(S_t)$ using the cross-correlation integral:

$$C_{XY}(r) = \frac{1}{N_{ref}N_t} \sum_{i=1}^{N_{ref}} \sum_{j=1}^{N_t} \theta(r - \|Y_i(S_{ref}) - X_j(S_t)\|) \quad (28)$$

Here, $\|\cdot\|$ denotes the Euclidian norm, and θ the Heaviside step function. N_{ref} and N_t are the number of points in the phase space of the reference and sliding windows, respectively. The distance r is usually defined as the 30% quintile of the cumulative neighborhood distribution of the reference window [36]. In order to further improve the discriminatory power between two dynamics, the autocorrelation integral $C_{XX}(r)$ and $C_{YY}(r)$ are used, the dynamical similarity index γ_{XY} is thus written as [17]:

$$\gamma_{XY} = \frac{C_{XY}}{\sqrt{C_{XX}C_{YY}}} \quad (29)$$

Dynamical similarity index provides a sensitive measure of closeness between two dynamics. If the reference and present window share the same underlying dynamics, the value of γ_{XY} is around 1, otherwise it goes down to 0.

3.2.3.6. Fuzzy similarity index. Fuzzy similarity index was extracted from dynamical similarity index by Ouyang et al. [17]. The concept of dynamical similarity index is hard or binary according to the Heaviside function. As a result, the data just outside the hyper sphere

are not accounted and all of the data inside the hyper sphere are treated equally. In the fuzzy similarity index, a Gaussian function is employed to replace the Heaviside function in the dynamical similarity; consequently, the hard boundary in the dynamical similarity becomes soft. The Gaussian function represents a fuzzy similarity between the neighbors and the points around. After replacing Heaviside function with Gaussian function, the correlation integral becomes:

$$C_{XY}^F(r) = \frac{1}{N_{ref}N_t} \sum_{i=1}^{N_{ref}} \sum_{j=1}^{N_t} \exp\left(-\|Y_i(S_{ref}) - X_j(S_t)\|^2 / r^2\right) \quad (30)$$

Fuzzy similarity index is then defined as:

$$\gamma_{XY}^F = \frac{C_{XY}^F}{\sqrt{C_{XX}^F C_{YY}^F}} \quad (31)$$

Similar to the Dynamical similarity index, if the reference and present window share the same underlying dynamics, the value of fuzzy similarity index is around 1, otherwise it goes down to 0.

3.2.3.7. Bhattacharyya based dissimilarity index (BBDI). In [10], a new dissimilarity index was proposed by the authors by inspiration of dynamical and fuzzy similarity indices and is referred to as BBDI in this paper. The concept of dynamical similarity index is hard or binary according to the Heaviside function. Fuzzy similarity index has been proposed to overcome this problem using Gaussian function instead of Heaviside function. However, both dynamical and fuzzy similarity indices need to determine a radius scale chosen according to the cumulative neighborhood distribution of the reference set that is challenging in these methods. In [10] the BBDI was proposed to overcome both the above-mentioned problems. The novelty of this method was the use of the Bhattacharyya distance. Bhattacharyya distance was employed to measure dynamical dissimilarity. BBDI can demonstrate the temporal distribution of changes from the epileptiform EEGs. The method consists of the reconstruction of EEG dynamics and the

measurement of dissimilarity between dynamics from a reference state and a present one (windowed EEG). Using the Bhattacharyya distance to calculate the dynamical dissimilarity index of the data points is neither hard nor binary and does not require adopting a proper radius scale because there is no radius scale in BBDI. Moreover, BBDI is computationally faster.

In this method, Bhattacharyya distance of $X(S_t)$ and $X(S_{ref})$ can be written as:

$$D_B(X(S_t), Y(S_{ref})) = \frac{1}{8} (m_{X(S_t)} - m_{Y(S_{ref})})^T P^{-1} (m_{X(S_t)} - m_{Y(S_{ref})}) + \frac{1}{2} \ln \left(\frac{\det(P)}{\sqrt{\det(P_{X(S_t)}) \det(P_{Y(S_{ref})})}} \right) \quad (32)$$

where $m_{X(S_t)}$ and $m_{Y(S_{ref})}$ are mean values of columns of the matrices $X(S_t)$ and $Y(S_{ref})$, and $P_{X(S_t)}$ and $P_{Y(S_{ref})}$ are covariance matrices of the matrices $X(S_t)$ and $Y(S_{ref})$, and $P = \frac{P_{X(S_t)} + P_{Y(S_{ref})}}{2}$.

If the reference and present window share the same underlying dynamics, BBDI has low values; otherwise, it increases.

4. Results

In this section, the results of analyzing the above-defined features and indices applied to the described dataset are presented.

4.1. First approach for detection (Thresholding)

ECoG signals of 6 rats in the test group and 15 rats in the control group were divided into segments; duration of each sliding window was 1 s (1000 points). Then, all 22 features and indices were examined.

Coastline and nonlinear energy features were successful in this approach. Fig. 2 shows the trend of coastline feature extracted from epileptiform ECoG data of a rat in the test group. Smoothed coastline

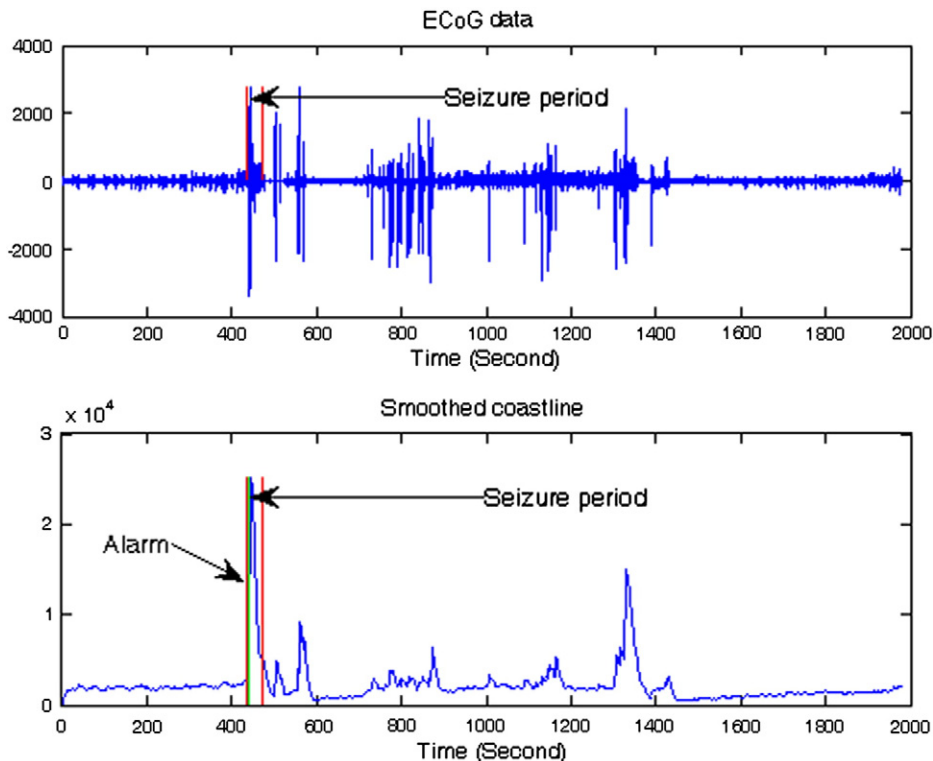


Fig. 2. Top: The long-term ECoG recordings of a rat in the test group. Bottom: The smoothed coastline values are plotted, which abruptly increase at the seizure onset. Red lines present seizure onset and end, respectively and green line presents alarm time. For this rat, delay of alarm is 3 s.

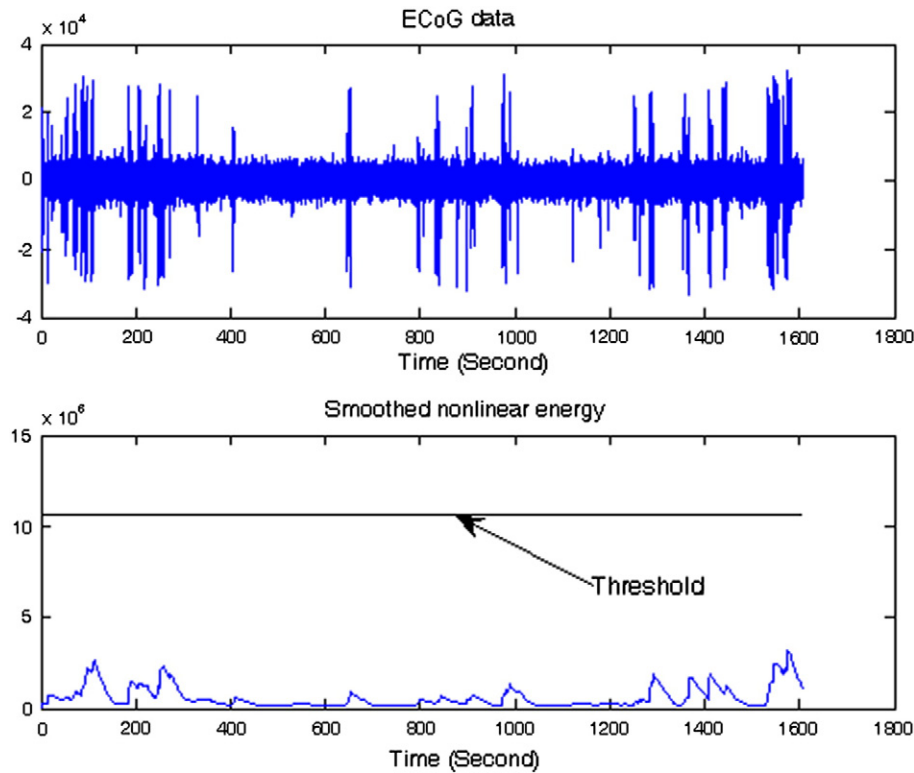


Fig. 3. Top: The long-term ECoG recording of a rat in the control group. Bottom: The smoothed nonlinear energy values fluctuations appear at the low level. The horizontal line represent the threshold of baseline for seizure onset detection of depth $k=5$ and $d=1$.

values are shown at the bottom of Fig. 2. It can be seen that coastline values are sensitive to quick and high fluctuations of ECoG but still remain within relatively small bounds before the seizure onset. On the contrary, coastline values sharply increase at seizure onset. Optimum performances for the seizure onset detection algorithms were obtained with values of $k=2.5$ and $d=3$ for coastline and values of $k=5$ and $d=1$ for nonlinear energy. Both coastline and nonlinear energy features had 1 false alarm in the test group and no false alarm in the control group. For both of them, sensitivity and specificity were 83% and 95%, and Q was 89% consequently.

Between these two features, the better result was achieved by coastline feature, which led to 2 ± 2 seconds delay in its correct detections. Nonlinear energy feature led to 3.6 ± 3.05 seconds delay in its correct detections. Fig. 3 (bottom) shows smoothed nonlinear energy values for a rat in the control group. It was observed that nonlinear energy values were at a low level during the long-term ECoG recording.

4.2. Second approach for detection (Classification)

In this section, again, all 22 features were examined. For similarity and dissimilarity indices, a long 100-second ECoG segment (100,000 points) during an interval quite distant in time from any seizure was selected as reference window. Fig. 4 summarizes the values of fuzzy similarity index of the 12 rats in the test group before, during, and after seizure periods. Based on the diagram, the fuzzy similarity index can efficiently detect induced seizures. The bars in Fig. 4 represent the average values of fuzzy similarity index before, during, and after seizure periods.

Statistical analysis is needed for each feature or index to determine whether its distributions over the three periods (before, during, and after seizure) are significantly different. To do this, the one-way analysis of variance (ANOVA) was performed on average of each feature or index values in the three periods.

The results for fuzzy similarity index are presented in Fig. 5. It is seen that the fuzzy similarity index values before and after seizure intervals are higher than of during seizure interval.

In order to more deeply test these observed mean differences statistically, in addition to the one-way ANOVA, Tukey's post-hoc test was also performed for each feature or index values of the three periods. Table 2 shows results for fuzzy similarity index.

P_{value} is considered as the criterion for seizure detection. Table 3 presents P_{value} s of all features and indices. Results show that dynamical similarity index, fuzzy similarity index, BBDI and also RR, ENTR and L in the recurrence plots led to $P_{value} < 0.05$. Therefore, they have significant variations before seizure and during seizure periods. BBDI

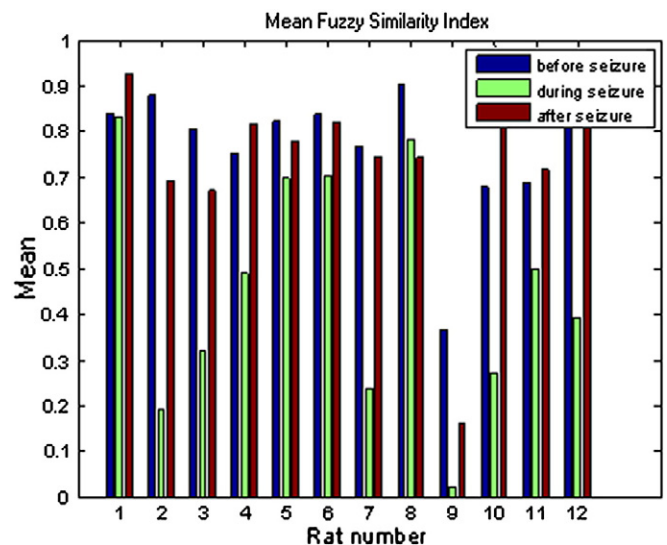


Fig. 4. Fuzzy similarity index of three periods. For all rats, the average values of fuzzy similarity index during seizure phase are lower than before and after seizure phases.

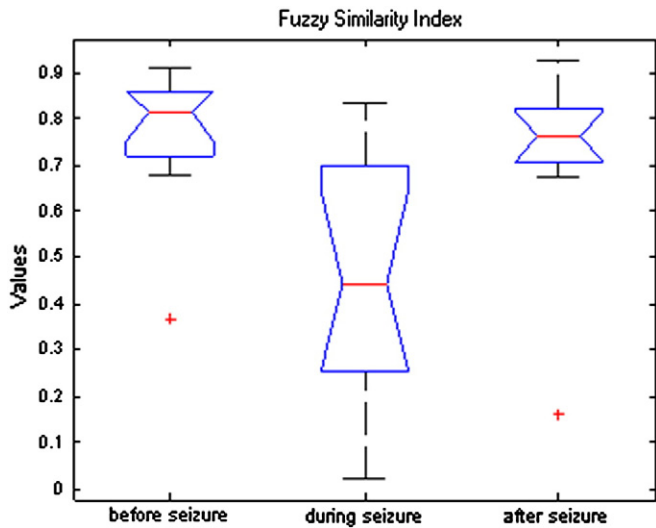


Fig. 5. The boxplot of fuzzy similarity index before, during and after seizure periods.

and L in the recurrence plots are used for the first time in this work for detecting induced seizures.

Dynamical and fuzzy similarity indices were able to pass Tukey's post-hoc test successfully. Therefore, not only are they able to discriminate before seizure and during seizure phases, they also are able to discriminate during seizure and after seizure phases. Between these two indices, fuzzy similarity index was more applicable because it discriminated more and led to a lower P_{value} ($P_{value} < 0.001$).

5. Discussion and conclusions

In this paper, a unified approach for detection of induced seizures in rats was presented. Common features and indices used for processing of single channel epileptiform EEGs for seizure detection were described. In this research, for the first time, nonlinear energy and coastline features were successfully employed for seizure onset detection, obtaining superior results compared with the results of other features and indices. BBDI and the value of average diagonal length in the recurrence plots that were used for the first time in

Table 2
One-way ANOVA with comparisons between the means using Tukey's test. Data are the fuzzy similarity index before, during, and after seizure phases.

Rat no	Before seizure	During seizure	After seizure
1	0.8401	0.831	0.9248
2	0.8776	0.1932	0.6906
3	0.8057	0.3203	0.6713
4	0.7522	0.4911	0.8172
5	0.8222	0.6969	0.7798
6	0.8369	0.7023	0.8191
7	0.7664	0.238	0.7439
8	0.9005	0.782	0.7431
9	0.3679	0.0227	0.1611
10	0.6794	0.2738	0.9127
11	0.6874	0.4983	0.7187
12	0.9063	0.3931	0.8273
Mean	0.7702	0.4535	0.7341

ANOVA source of variation	Sums of squares (SS)	Degrees of freedom (DF)	Mean square (MS)	F	Prob>F
Treatment	0.7213	2	0.3606	8.54	0.001
Error	1.3938	33	0.0422		
Total	2.1151	35			

Tukey test: before seizure phase vs. during seizure phase $q = 5.337$ ($P < 0.01$), after seizure phase vs. during seizure phase $q = 4.729$ ($P < 0.01$).

Table 3
 P_{value} s of all features and indices for detection of induced seizures.

Feature or Index	P_{value}	Feature or Index	P_{value}
Approximate Entropy	0.0503	Nonlinear Energy	0.5593
Fractal Dimension	0.5728	Activity	0.7762
Lyapunov exponent	0.1165	Dynamical Similarity Index	0.0034
Complexity	0.0635	Fuzzy Similarity Index	0.001
Mobility	0.8881	BBDI	0.0089
Spectral Entropy	0.2471	RR	0.0227
Spectral Kurtosis	0.174	DET	0.3704
Spectral Skewness	0.181	ENTR	0.0157
Coastline	0.7416	L	0.0061
Autocorrelation	0.742	LAM	0.5339
Normalized Autocorrelation	0.5989	TT	0.0772

this study were successful in classification approach of seizure detection in rats. However, dynamical and fuzzy similarity indices, which had been already used, led to better results in this approach.

The main advantage of this work is that several features in different categorizations have been examined. Moreover, both possible approaches for seizure detection have been considered. The dataset in this work includes more rats in comparison to other datasets [45–47,49–52]. Moreover, most of the previous studies in the area of PTZ-induced seizure detection employed only one, two or three features and they considered only one approach for seizure detection.

Application of a wide range of features with different levels of complexity and sensitivity can reveal suitability of each feature in each approach for detecting PTZ-induced seizures. However, as a limitation of this work, the features have been examined separately, so that in future studies, the suitable features in each approach should be put in a feature vector and employed together.

According to the results of this study, variance-based features such as nonlinear energy and coastline are more appropriate for tracking abrupt changes in ECoG (or EEG) signal. Therefore, these two features perform better in thresholding approach. The other features are slower and less sensitive. The results show that nonlinear features or indices, which are based on dynamical system theories, can better track transition of a neural system from seizure-free to ictal period. Among these features or indices, two groups of features or indices had significantly better results: similarity or dissimilarity indices and RQA features. Similarity or dissimilarity indices can better track transition from interictal period to ictal period since they compare present window to a reference window in the interictal period. RQA that was also widely used in this study has significant advantages such as no assumption about noise, linearity, stationarity and length of signal. Therefore, it is a suitable tool for analysis of ECoG (or EEG) signals.

Perspectives include application of a larger number of sophisticated features or indices and combination of suitable features or indices in each approach to improve the performance of seizure detection.

Acknowledgment

The authors would like to thank Mr. Tyley Kaster from Schulich School of Medicine and Dentistry, University of Western Ontario, for his assistance in editing the paper.

References

- [1] Firpi H, Goodman ED, Echuaz J. Epileptic seizure detection using genetically programmed artificial features. *IEEE Trans Biomed Eng* 2007;54(2):212–24.
- [2] Lehnertz K, Mormann F, Kreuz T, et al. Seizure prediction by nonlinear EEG analysis. *IEEE Eng Med Biol Mag* 2003;22:57–63.
- [3] Srinivasan V, Eswaran C, Siraam N. Approximate entropy-based epileptic EEG detection using artificial neural networks. *IEEE Trans Inf Technol Biomed* 2007;11(3):288–95.

- [4] Schelter B, Winterhalder M, Maiwald T, et al. Testing statistical significance of multivariate time series analysis techniques for epileptic seizure prediction. *Chaos* 2006;16:013108.
- [5] Adeli H, Ghosh-Dastidar S, Dadmehr N. A wavelet-chaos methodology for analysis of EEGs and EEG subbands to detect seizure and epilepsy. *IEEE Trans Biomed Eng* 2007;54(2):205–11.
- [6] Gotman J. Automatic recognition of epileptic seizures in the EEG. *Electroencephalogr Clin Neurophysiol* 1982;54(5):530–40.
- [7] Esteller R. "Detection of seizure onset in epileptic patients from intracranial EEG signals." Ph.D. dissertation, Dept. Electrical Eng., Georgia Inst. Tech., Atlanta, GA, 1999.
- [8] Gotman J. Automatic seizure detection: improvements and evaluation. *Electroencephalogr Clin Neurophysiol* 1990;76:317–24.
- [9] Kalayci T, Ozdamar O. Wavelet preprocessing for automated neural network detection of EEG spikes. *IEEE Eng Med Biol Mag* 1995:160–6.
- [10] Niknazar M, Mousavi SR, Vosoughi Vahdat B, Shamsollahi MB, Sayyah M. A new dissimilarity index on EEG signals for epileptic seizure detection. 4th International Symposium on Communications, Control and Signal Processing (ISCCSP 2010), Cyprus; 2009.
- [11] Mousavi SR, Niknazar M, Vahdat BV. Epileptic seizure detection using AR model on EEG signals. Biomedical engineering conference, 2008. CIBEC 2008. Egypt: Cairo International; 2008.
- [12] Adeli H, Zhou Z, Dadmehr N. Analysis of EEG records in an epileptic patient using wavelet transform. *J Neurosci Methods* 2003;123(1):69–87.
- [13] Andrew GJ, Seyal M. Automated interictal EEG spike detection using artificial neural networks. *Electroencephalogr Clin Neurophysiol* 1992;83:271–80.
- [14] Webber WRS, Litt B, Wilson K, Lesser RP. Practical detection of epileptiform discharges (EDs) in the EEG using an artificial neural network: a comparison of raw and parameterized EEG data. *Electroencephalogr Clin Neurophysiol* 1994;91:194–204.
- [15] Iasemidis LD, Olson LD, Sackellares JC, Savit RS. Time dependencies in the occurrences of epileptic seizures: A nonlinear approach. *Epilepsy Res* 1994;17:81–94.
- [16] Li X, Ouyang G, Yao X, Guan X. Dynamical characteristics of pre-epileptic seizures in rats with recurrence quantification analysis. *Phys Lett A* 2004;333:164–71.
- [17] Ouyang G, Li X, Guan X. Use of fuzzy similarity index for epileptic seizure prediction. The 5th world congress on intelligent control and automation, Hang Zhou, China, June 14–18; 2004. p. 5351–5.
- [18] Loscher W, Schmidt D. Which animal models should be used in the search for new antiepileptic drugs? A proposal based on experimental and clinical considerations. *Epilepsy Res* 1988;2:145–81.
- [19] Ouyang G, Li X, Dang C, Richards D. Using recurrence plot for determination analysis of EEG recordings in genetic absence epilepsy rats. *Elsevier Clinical Neurobiology*, vol. 119; 2008. p. 1747–55.
- [20] Danober L, Deransart C, Depaulis A, Vergne M, Marescaux C. Pathophysiological mechanisms of genetic absence epilepsy in the rat. *Prog Neurobiol* 1998;55:27–57.
- [21] Paivinen N, Lammi S, Pitkanen A, Nissinen J, Penttonen M, Gronfors T. Epileptic seizure detection: A nonlinear viewpoint. *Comput Methods Programs Biomed* 2005;79(2):151–9.
- [22] White AM, Williams PA, Ferraro DJ, et al. Efficient unsupervised algorithms for the detection of seizures in continuous EEG recordings from rats after brain injury. *J Neurosci Methods* 2006;152:255–66.
- [23] Shannon CE. A mathematical theory of communication. *Bell Syst Tech J* 1948;27:379–423.
- [24] Thomasson N, Hoepfner T, Webber C, Zbilut J. Recurrence quantification in epileptic EEGs. *Phys Lett A* 2001;279:94–101.
- [25] Elsner JB, Tsonis AA. Singular spectrum analysis: a new tool in time series analysis. New York: Plenum; 1996.
- [26] Marwan N, Wessel N, Meyerfeldt U, Kurths Jürgen. Recurrence plots for the analysis of complex systems. *Physics Reports*, vol. 438; 2007. p. 237–329.
- [27] Fraser AM, Swinney H. Independent coordinates for strange attractors. *Phys Rev* 1986;A33:1134–40.
- [28] Cao L. Practical method for determining the minimum embedding dimension of a scalar time series. *Physica D* 1997;110(1–2):43–50.
- [29] Casdagli M. Recurrence plot revisited. *Physica D* 1997;108:12–44.
- [30] Eckmann JP, Kamphorst SO, Ruelle D. Recurrence plots of dynamical systems. *Europhys Lett* 1987;4(8):973.
- [31] Mormann F, Andrzejak RG, Kreuz T, et al. Automated detection of a pre-seizure state based on a decrease in synchronization in intracranial electroencephalogram recordings from epilepsy patients. *Phys Rev E* 2003;67:021912 [1–10].
- [32] Accardo A, Affinito M, Carozzi M, Bouquet F. Use of the fractal dimension for the analysis of electroencephalographic time series. *Biol Cybern* 1997;77:339–50.
- [33] Pincus SM, Gladstone IM, Ehrenkrantz RA. A regularity statistic for medical data analysis. *J Clin Monit* 1991;7:335–45.
- [34] Kantz H, Schreiber T. Nonlinear time series analysis. Cambridge: Cambridge University Press; 1997.
- [35] Quyen MLV, Martinerie J, Navarro V, Boon P, D'Have M, Adam C, Renault B, Varela F, Baulac M. Anticipation of epileptic seizures from standard EEG recordings. *Lancet* 2001;357:183–8.
- [36] Quyen MLV, Adam C, Martinerie J, Baulac M, Clemencau S, Varela F. Spatio-temporal characterization of non-linear changes in intracranial activities prior to human temporal lobe seizures. *Eur J Neurosci* 2000;12:2124–34.
- [37] Feldwisch-Drentrup H, Schelter B, Jachan M, Nawrath J, Timmer J, Schulze-Bonhage A. Joining the benefits: combining epileptic seizure prediction methods. *Epilepsia* 2010;51:1598–606.
- [38] Harris B, Gath I, Rondouin G, Feuerstein C. On time delay estimation of epileptic EEG. *IEEE Trans Biomed Eng* 1994;41(9):820–9.
- [39] Guler I, Kiyimik MK, Akin M, Alkan A. AR spectral analysis of EEG signals by using maximum likelihood estimation. *Comput Biol Med* 2001;31:441–50.
- [40] Haykin S. *Neural Network: A comprehensive foundation*. 2nd ed. Pearson Education; 2004.
- [41] Fisher RS, Boas WVE, Blume W, et al. Epileptic seizures and epilepsy: definitions proposed by the International League Against Epilepsy (ILAE) and the International Bureau for Epilepsy (IBE). *Epilepsia* 2005;46:470–2.
- [42] Koivuluoma M, Huupponen E, Varri A, Olejarczyk E, Klonowski W. Comparison of some linear and non-linear methods in the quantification of NREM sleep process. Proceedings of international symposium on nonlinear theory and its applications, vol. 200. NOLTA; 2001. p. 411–4.
- [43] Niknazar M, Vahdat BV, Shamsollahi MB, Sayyah M. Application of Bhattacharyya distance as a dissimilarity index for automated prediction of epileptic seizures in rats. International Conference on Intelligent and Advanced Systems (ICIAS), Malaysia; 2010.
- [44] Besio WG, Liu X, Liu Y, Sun YL, Medvedev AV, Koka K. Algorithm for automatic detection of pentylenetetrazole-induced seizures in rats. Proc. 33rd Annu. Int. Conf. IEEE EMBS, Boston, MA; 2011. p. 8283–6.
- [45] Feltane A, Boudreaux-Bartels GF, Besio W. Automatic seizure detection in rats using Laplacian EEG and verification with human seizure signals. *Ann Biomed Eng* 2012. <http://dx.doi.org/10.1007/s10439-012-0675-4>.
- [46] Sherman D, Zhang N, Garg S, et al. Detection of nonlinear interactions of EEG alpha waves in the brain by a new coherence measure and its application to epilepsy and anti-epileptic drug therapy. *Int J Neural Syst* 2011;21(2):115–26.
- [47] Harreby KR, Sevcencu C, Struijk JJ. Early seizure detection in rats based on vagus nerve activity. *Med Biol Eng Comput* 2011;49:143–51.
- [48] Eberle MM, Reynolds CL, Szu JJ, et al. In vivo detection of cortical optical changes associated with seizure activity with optical coherence tomography. *Biomed Opt Express* 2012;3(11):2700–6.
- [49] Paul J, Patel C, Al-Nashash H, et al. Prediction of PTZ-induced seizures using wavelet-based residual entropy of cortical and subcortical field potentials. *IEEE Trans Biomed Eng* 2003;50:640–8.
- [50] Moxon KA, Kuzmick V, Lafferty J, et al. Real-time seizure detection system using multiple single-neuron recordings. Proc. of the 23rd Annual International Conference of the IEEE Engineering in Medicine and Biology Society, Istanbul, Turkey, October 25–28, 2001; 2001.
- [51] Fanselow EE, Reid AP, Nicoletis MAL. Reduction of pentylenetetrazole-induced seizure activity in awake rats by seizure-triggered trigeminal nerve stimulation. *J Neurosci* 2000;20:8160–8.
- [52] Makeyev O, Liu X, Luna-Munguia H, et al. Toward a noninvasive automatic seizure control system in rats with transcranial focal stimulations via tripolar concentric ring electrodes. *IEEE Trans Neural Syst Rehabil Eng* 2012;20(4):422–31.
- [53] Makeyev O, Liu X, Luna-Munguia H, et al. Toward an automatic seizure control system in rats through transcranial focal stimulation via tripolar concentric ring electrodes. Proc. 65th Annual Meeting of the American Epilepsy Society, vol. 12, no. s1. , *Epilepsy Currents*; 2012. p. 29–30.
- [54] Racine RJ. Modification of seizure activity by electrical stimulation: II. Motor seizure. *Electroencephalogr Clin Neurophysiol* 1972;32(3):281–94.
- [55] Abramowitz M, Stegun IA, editors. *Handbook of mathematical functions: with formulas, graphs, and mathematical tables*, vol. 55. Dover Publications; 1965.
- [56] Rho MJ, Sankar R, Stafstrom CE. *Epilepsy: mechanisms, models, and translational perspectives*. CRC Press; 2010.
- [57] Wendling F, Bartolomei F, Senhadji L. Spatial analysis of intracerebral electroencephalographic signals in the time and frequency domain: identification of epileptogenic networks in partial epilepsy. *Philos Trans R Soc A Math Phys Eng Sci* 2009;367(1887):297–316.
- [58] Stables JP, Bialer M, Johannessen SI, et al. Progress report on new antiepileptic drugs A summary of the Second Eilat Conference. *Epilepsy Res* 1995;22(3):235–46.
- [59] Mirski MA, Tsai YC, Rossell LA, Thakor NV, Sherman DL. Anterior thalamic mediation of experimental seizures: selective EEG spectral coherence. *Epilepsia* 2003;44(3):355–65.
- [60] Klioueva IA, van Luijckelaar ELJM, Chepurnova NE, Chepurnova SA. PTZ-induced seizures in rats: effects of age and strain. *Physiol Behav* 2001;72(3):421–6.
- [61] De Deyn PP, D'Hooge R, Marescau B, Pei YQ. Chemical models of epilepsy with some reference to their applicability in the development of anticonvulsants. *Epilepsy Res* 1992;12(2):87–110.